



## Original Article

# MiR-590-3p affects the function of adipose-derived stem cells (ADSCs) on the survival of skin flaps by targeting VEGFA

Kai Yang, Xiancheng Wang<sup>\*</sup>, Yang Sun, Xiang Xiong, Xianxi Meng, Bairong Fang, Wenbo Li, Zhongjie Yi

Department of Plastic Surgery and Burns Surgery, The Second Xiangya Hospital, Central South University, Changsha, Hunan 410011, China

## ARTICLE INFO

## Article history:

Received 1 March 2022

Received in revised form

28 May 2022

Accepted 23 July 2022

## Keywords:

Skin flap

Adipose-derived stem cells

Flap survival

miR-590-3p

VEGFA

## ABSTRACT

**Introduction:** Partial necrosis of skin flaps is still a substantial problem in plastic and reconstructive surgery. In this study, the role of miR-590-3p in adipose-derived stem cells (ADSCs) transplantation in improving the survival of skin flap in a mouse model was delved into.

**Method:** An abdominal perforator flap model was established in mice. The histopathological examination of mice skin tissues after ADSCs transplantation was implemented using Hematoxylin & eosin (H&E) staining. Immunohistochemistry (IHC) or immunofluorescence (IF) staining was utilized to assess the PCNA or CD31 levels. The concentrations of VEGFA in the culture medium were quantified using a VEGFA ELISA kit.

**Result:** The damage of tissue in the skin flap was dramatically relieved by ADSCs transplantation. MiR-590-3p overexpression notably suppressed, while miR-590-3p knockdown facilitated skin flap survival by regulating PCNA, VCAM-1, and VEGFA levels. MiR-590-3p targeted VEGFA to regulate its expression. The knockdown of VEGFA significantly inhibited, while overexpression of VEGFA notably promoted the survival of skin flap.

**Conclusion:** ADSCs transplantation promotes skin flap survival by boosting angiogenesis. The miR-590-3p/VEGFA axis modulates skin flap angiogenesis and survival in ADSCs. These results reveal that interfering with miR-590-3p in ADSCs could potentially be a novel therapeutic target for the improvement of skin flap survival.

© 2022, The Japanese Society for Regenerative Medicine. Production and hosting by Elsevier B.V. This is an open access article under the CC BY-NC-ND license (<http://creativecommons.org/licenses/by-nc-nd/4.0/>).

## 1. Introduction

Transplantation of skin flap is a common procedure in plastic and reconstructive surgery [1,2]. However, numerous complications are entailed by this procedure, such as partial flap necrosis, insufficient neovascularization, and reduced proangiogenic factor production levels [3–5]. Flap necrosis can be exacerbated by harmful changes in the tissue and vasculature that mostly stem

from insufficient blood perfusion and ischemia-reperfusion injury [6]. Therefore, the increase of proangiogenic factor levels, angiogenesis, and the decrease of necrosis which helps to improve skin flap survival, and the possibility of successful skin transplantation should be prioritized.

Boosting flap survival by stem cell therapy has garnered widespread academic interest [7]. Adipose-derived stem cells (ADSCs), a stem cell population in the adipose tissue, have much differentiation potential [8,9]. Therapeutic cell transplantation of ADSCs has recently been identified as an efficient method for restoring tissue vascularization after ischemic events [10]. Some experimental studies revealed that the use of ADSCs potentially contributes to boosting flap angiogenesis, showing substantial clinical application potentials [11–13]. Regarding action mechanisms, ADSCs secrete several growth factors (such as VEGF, TGF- $\beta$ , and PDGF), promoting angiogenesis in wound healing. Moreover, IL-6 plays a protective role in the usage of ADSCs of skin flaps against ischemia/

**Abbreviations:** ADSCs, Adipose-derived stem cells; miRNAs, MicroRNAs; UTR, Untranslated region; H&E, Hematoxylin & eosin; IHC, Immunohistochemistry; IF, Immunofluorescence; RIPA, Radioimmunoprecipitation assay; RIP, Argonaute2 RNA immunoprecipitation; ELISA, Enzyme-linked immunosorbent assay.

<sup>\*</sup> Corresponding author. Department of plastic surgery and burns surgery, The Second Xiangya Hospital, Central South University, China.

E-mail address: [wangxiancheng64@csu.edu.cn](mailto:wangxiancheng64@csu.edu.cn) (X. Wang).

Peer review under responsibility of the Japanese Society for Regenerative Medicine

<https://doi.org/10.1016/j.reth.2022.07.010>

2352-3204/© 2022, The Japanese Society for Regenerative Medicine. Production and hosting by Elsevier B.V. This is an open access article under the CC BY-NC-ND license (<http://creativecommons.org/licenses/by-nc-nd/4.0/>).

reperfusion injury [11,14]. However, the mechanism of the ADSCs in skin flaps remains unclear as of yet.

MicroRNAs (miRNAs), a general group of short non-coding single-stranded RNAs, post-transcriptionally modulate human genetic expression level by combining with the 3'-untranslated region (UTR) of targeted mRNAs, thereby inducing mRNA translational degradation/repression [15]. Moreover, numerous studies have revealed that a flock of miRNAs play vital roles in the usage of ADSCs and skin morphogenesis and regeneration. For example, Shi et al. reported that miR-128-3p affects ADSCs to inhibit wound healing in diabetic mice by regulating SIRT1-mediated autophagy [16]. Li et al. demonstrated that miR-150 modulates adipogenic differentiation of ADSCs by targeting Notch3 [17]. Moreover, miR-590-3p was shown, in our previous study, to suppress ADSCs secreting VEGFA through binding to VEGFA 3'UTR, thereby inhibiting angiogenesis [18]. Nevertheless, the biological function of miR-590-3p in the application of ADSCs of skin flaps has not been fully clarified.

In this study, the biological functions and the potential mechanism of miR-590-3p in ADSC transplantation to the skin flap, along with ADSCs protective impacts on flap survival, were revealed. It was revealed that overexpressed miR-590-3p dramatically inhibited skin flap survival through the regulation of VEGFA. Based upon these results, miR-590-3p is a potentially promising target in flap therapy.

## 2. Materials and methods

### 2.1. Experimental animals

BALB/c mice (8 weeks, female) supplied by Hunan SJA Laboratory Animal Co., Ltd (Changsha, China) were fed in a temperature-maintained room with a stabilized temperature of  $25\text{ }^{\circ}\text{C} \pm 2\text{ }^{\circ}\text{C}$ , a moisture capacity of 50%–70% air and a stable 12h light/12h dark cycle at a specific pathogen-free level. The use of animals was authorized by The Second Xiangya Hospital of Central South University (Approval of animal Ethic Number 2021271).

### 2.2. ADSC culture, and identification

Primary human ADSCs were purchased from OriCell® Cyagen (Guangzhou, China) and cultured in human ADSC complete culture medium (Cyagen). Flow cytometry (NovoCyte, Angilent, USA) was utilized for the analysis of ADSC immunophenotypes (CD90, CD29, CD13, CD31, CD34, and CD45). Oil red O staining was utilized to verify adipogenic differentiation according to previous studies (Fig. S1). ADSCs underwent a culture in 95% air (20% O<sub>2</sub>) and 5% CO<sub>2</sub> allowing cell passage for 2–4 generations.

### 2.3. Flap animal model and experimental design

Mouse anesthesia was finished via the intraperitoneal injection of 2% (w/v) pentobarbital sodium (40 mg/kg, Sigma–Aldrich), an abdominal perforator flap ( $2 \times 3\text{ cm}^2$ ) was constructed as reported previously [19]. Briefly, borders of the skin paddle were incised down to the rectus fascia. The skin flap was elevated from lateral to medial on both sides, beneath the panniculus carnosus. The flap was based on a single perforator vessel from the left rectus abdominis muscle. Then, the flap was sutured back to its original position. For the sham group, incisions at the same site were performed and then sutured *in situ*. After surgery, the mice were received a subcutaneously injection of Carprofen (5 mg/kg, once per day for 3 days) to relieve pain.

A total of 50 mice were randomly grouped (sham, perforator flap, and perforator flap + ADSCs, perforator flap + agomir-NC

transfected ADSCs, perforator flap + agomir-590-3p transfected ADSCs, perforator flap + antagomir-NC transfected ADSCs, perforator flap + antagomir-590-3p transfected ADSCs, perforator flap + si-NC transfected ADSCs, perforator flap + si-VEGFA transfected ADSCs, perforator flap + rVEGFA protein (2 μg, sinobiological, China) plus ADSCs, 5 mice for each. In groups with ADSCs transplantation, ADSCs ( $1 \times 10^6$  cells) were suspended in 100 μl DMEM, followed by injection into subcutaneous tissues. The flap showed an elevation at 10 points from bottom to distal along the flap axis. Mice injected with 100 μl DMEM before operation served as control.

### 2.4. Flap evaluation

Flap survival and macroscopic changes (appearance, color, texture, and hair condition) within 7 days were observed. The survival area was measured by caliper. The mice were euthanized on day 7. The flaps were collected. About  $1 \times 1\text{ cm}^2$  of central tissue from each flap was collected for histological analysis and Western blot analysis.

### 2.5. ADSC transfection

The synthesis of agomir-NC, agomir-590-3p, antagomir-NC, and antagomir-590-3p were performed by GenePharma (Shanghai, China). VEGFA knockdown was achieved by transfection of si-VEGFA (at a final concentration of 100 nM GeneChem, Guangzhou, China). The overexpression or knockdown of miR-590-3p was achieved by transfection of agomir-590-3p or antagomir-590-3p (at a final concentration of 50 nM) into ADSCs with the help of Lipofectamine 2000 (Invitrogen). The sequences were shown in Table S1.

### 2.6. Hematoxylin & eosin (HE) staining

HE staining was utilized for the histopathological examination of mouse skin tissues. The skin tissue samples were fixed in a 4% formalin solution (4 °C, 8h), placed in a 70% ethanol solution (5 min), and applied for dehydration of gradient ethanol. The tissues were subsequently subjected to 30-min immersion in xylene and paraffin embedding. Skin tissues were continuously sliced into coronal sections (4 μm). After deparaffinization, the slices were subjected to HE staining. The samples were then observed and photographed under a light microscope (Olympus, Tokyo, Japan).

### 2.7. Immunohistochemistry (IHC)

IHC staining was performed on mouse skin tissue sections (4 μm). The tissues were mainly paraffin-embedded. After deparaffinization and rehydration using graded alcohols, the sections underwent 2 washes in PBS, 10 min each. Next, the sections were subjected to overnight incubation with rabbit polyclonal primary antibody of PCNA (Cat# ab29, 1/10000, Abcam, Cambridge, MA, USA), followed by 30-min incubation (37 °C) with secondary antibody horseradish peroxidase (HRP)-labeled goat polyclonal anti-mouse immunoglobulin G (IgG) H&L (1:500, ab6789, Abcam). After 3-min staining with 3, 3'-diaminobenzidine solution and then 10-min water washing, the sections were counterstained with hematoxylin, followed by 10-min rewashing using water. Finally, after dehydration and clearance, the sections were observed under a light microscope (Olympus, Tokyo, Japan).

### 2.8. Immunofluorescence (IF) staining

IF was performed on paraffin sections of mice skin tissues to detect the CD31 level. The sections underwent an overnight

incubation (4°C) with primary antibodies against CD31 (Cat# ab222783, 1/100, Abcam) after the standard dewaxing process, followed by 2-h incubation (room temperature) with a secondary Cy5-labeled antibody. They were then incubated (10 min, room temperature) with DAPI. Finally, the sections were covered, and a fluorescence microscope was used for observation.

### 2.9. Quantitative RT-PCR

Cell/tissue total RNA was extracted using TRIZOL™ (Invitrogen, Carlsbad, CA, USA), of which 2.0 µg was used for the synthesis of reverse transcription utilizing PrimeScript® Stra Strand Synthesis Kit (TaKaRa, Tokyo, Japan). The QuantiTect® SYBR® Green RT-PCR Kit (QIAGEN, Dusseldorf, Germany) was used in quantitative PCR. The  $2^{-\Delta\Delta Ct}$  method was used to calculate miR-590-3p and VEGFA expression, with U6 (for miRNAs) and GAPDH (for mRNA) as the internal reference.

### 2.10. Western blot

Radioimmunoprecipitation assay (RIPA) lysate (Beyotime, Shanghai, China) was used for cell/tissue total protein extraction. The bicinchoninic acid was utilized for quantitative analysis. The total protein (50–100 µg) subsequently underwent SDS-polyacrylamide gel electrophoresis for separation and then transferred onto polyvinylidene difluoride (PVDF) membranes. After 1-h blocking with TBS-T buffer with 5% nonfat milk, the membranes underwent an overnight incubation (4 °C) with primary antibody anti-PCNA (Cat# ab29, 1/1000, Abcam), and then 3 TBST washes, followed by a 1.5 h incubated with HRP-labelled secondary antibody rabbit anti-mouse IgG H&L (Cat# ab205719, 1:5000, Abcam) at room temperature. An ECL system (Life technologies corporation, Gaithersburg, MD, USA) was utilized for signal detection. The blot bands were captured by the Tannon chemiluminescence imaging system (Tannon, Shanghai, China).

### 2.11. Argonaute2 RNA immunoprecipitation (RIP) assay

Magna RIP RNA-Binding Protein Immunoprecipitation Kit (Millipore, USA) was used in the RIP assay. After the collection and cultivation in RIP lysis buffer, ADSCs ( $1 \times 10^7$  cells) were immunoprecipitated with Ago2 antibody (Cell Signaling Technology, MA, USA). Normal mouse IgG served as the controls. Then, the levels of miR-590-3p and 3'UTR of VEGFA in the immunoprecipitation were determined by real-time PCR.

### 2.12. Enzyme-linked immunosorbent assay (ELISA)

VEGFA concentration in the culture medium was quantified using a human VEGFA ELISA kit (Cat# ab119566, Abcam) according to the instruction. A multi-function microplate reader (BD, USA) was employed for determining the colorimetric optical densities (OD).

### 2.13. Statistical analysis

At least three independent experiments were conducted, respectively. Data were expressed as mean  $\pm$  SD. SPSS20.0 software was applied for statistical analysis. Differences between the two groups were contrasted using Student's t-test, and those among multiple groups were analyzed using one-way ANOVA followed turkey post-hoc test.  $P < 0.05$  was deemed a statistically significant difference.

## 3. Results

### 3.1. ADSCs transplantation enhances skin flap survival

A mouse model with abdominal perforator flap was established to explore ADSC effects on the perforator flaps (Fig. 1A). The perforator flap group displayed notably reduced survival area relative to the sham group, while ADSCs transplantation increased the skin flap survival area (Fig. 1B). H&E staining was carried out for skin flap histologic evaluation (Fig. 1C). When compared to the perforator flap group, ADSC transplantation notably reduced inflammation areas, caused more intact epithelialization, and increased hair follicles. IHC staining revealed that compared to the sham group, the proliferation-related protein PCNA expression level was notably reduced, while ADSCs transplantation elevated the PCNA level (Fig. 1D). IF staining indicated that CD31 expression was observably decreased in the perforator flap group, while ADSCs transplantation increased CD31 expression (Fig. 1E), indicating the blood vessels increased. Moreover, Western blot showed that VCAM-1 and VEGFA levels were decreased in the perforator flap group, while ADSCs transplantation enhanced VCAM-1 and VEGFA expression (Fig. 1F). All the above findings suggest that the damage of tissue in the perforator flap was dramatically relieved by ADSCs transplantation.

### 3.2. The impact of miR-590-3p regulates ADSCs on skin flap survival

To explore the specific functions of miR-590-3p regulating ADSCs on perforator flap survival, agomir-590-3p/antagomir-590-3p was transfected into ADSCs. The transfection efficiency was verified by a PCR assay (Fig. 2A). The outcomes reflected that agomir-590-3p dramatically upregulated miR-590-3p while antagomir-590-3p substantially downregulated miR-590-3p. The transfected ADSCs were subsequently injected into the subcutaneous tissue of the skin flap model mice, and agomir-590-3p inhibited, while antagomir-590-3p promoted the survival of the perforator flap (Fig. 2B). H&E staining results revealed that the skin tissues in the agomir-590-3p group exhibited larger inflammation areas and more fragmentary epithelialization, and fewer hair follicles. In comparison, the agomir-590-3p treatment caused opposite results (Fig. 2C). IF staining uncovered overexpressed miR-590-3p observably restrained, while it silenced miR-590-3p facilitated CD31 expression (Fig. 2D). Furthermore, the overexpression of miR-590-3p was markedly inhibited, while the silencing of miR-590-3p promoted PCNA, VCAM-1, and VEGFA protein levels (Fig. 2E).

### 3.3. MiR-590-3p targeted VEGFA regulates its expression

Our previous research verified the preliminary relationship of miR-590-3p and VEGFA; miR-590-3p targeting VEGFA 3'UTR was verified through luciferase reporter gene assay in 293T cells [18]. Furthermore, in this study, agomir-590-3p/antagomir-590-3p was transfected into ADSCs, and the VEGFA protein level in cells and culture medium was detected by a Western blot (Fig. 3A) and an ELISA (Fig. 3B) assay. Overexpression of miR-590-3p markedly inhibited, while miR-590-3p inhibition facilitated VEGFA expression levels and secretion (Fig. 3A and B). The RIP assay results showed that miR-590-3p and 3'UTR of VEGFA were enriched in the Ago2 immunoprecipitation that further confirmed miR-590-3p could targeted 3'UTR of VEGFA (Fig. 3C). Moreover, the influence of miR-590-3p and/or VEGFA knockdown in ADSCs in VEGFA expression was detected using a Western blot (left) and an ELISA

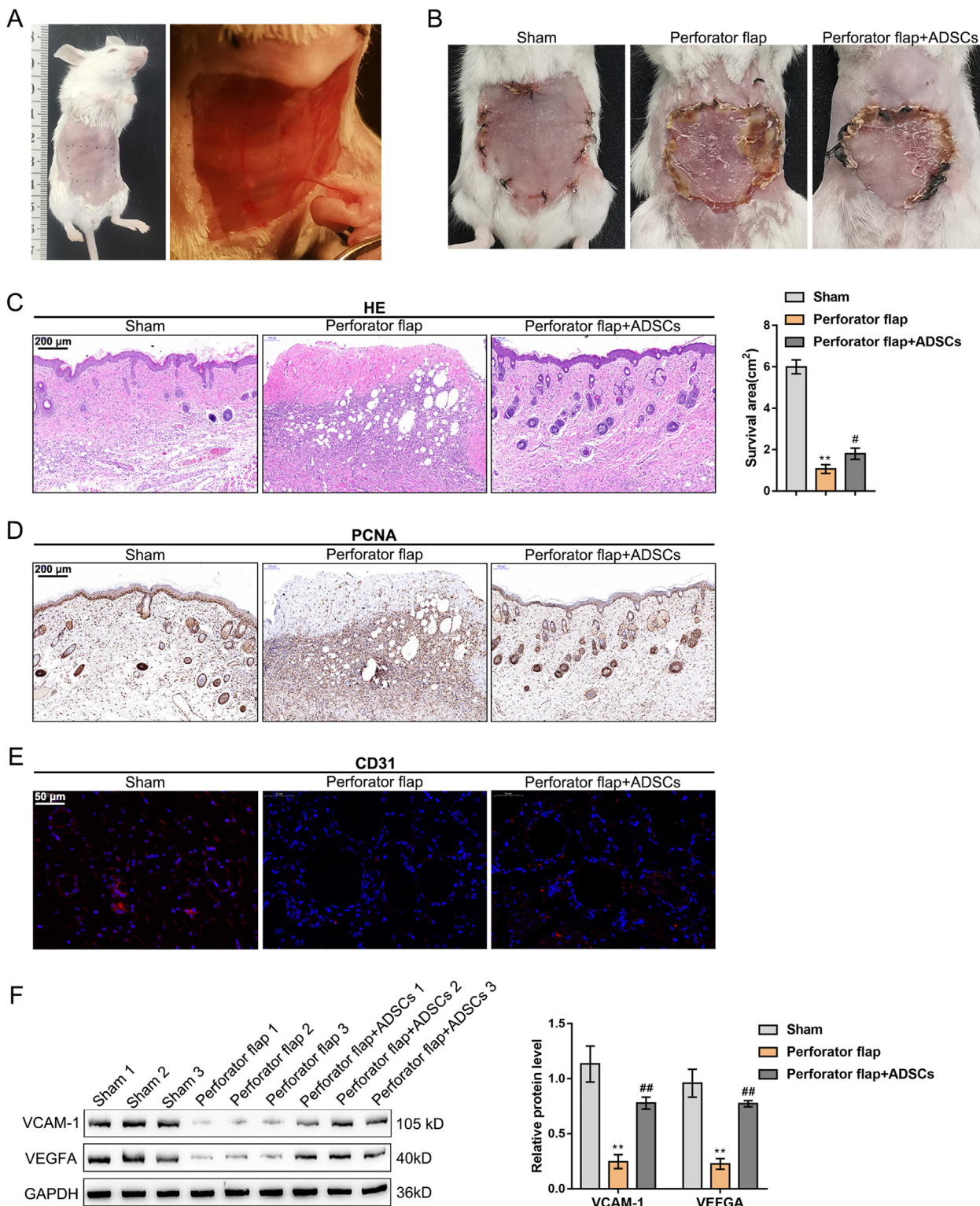


**Fig. 1. ADSC transplantation improves skin flap survival** (A) The abdominal perforator flap (B) Mice were grouped at random (sham, perforator flap, and perforator flap + ADSCs). Representative flap images on the 7th day after operation and statistical analysis of the survival area (C) The assessment of skin tissue damage was applied by H&E staining (D) The expression level of PCNA in skin tissue was detected by IHC staining (E) The expression level of CD31 in skin tissue was detected by IF staining (F) The protein levels of VCAM-1 and VEGFA in skin tissue were determined using Western blot. N = 5; \*\*P < 0.01, compared with Sham group; #P < 0.05, ##P < 0.01, compared with perforator flap group.

assay (right) (Fig. 3D). MiR-590-3p silencing observably increased, while VEGFA knockdown significantly inhibited VEGFA expression level. The impact of silencing miR-590-3p and VEGFA on VEGFA expression was shown to offset each other.

### 3.4. The effect of VEGFA regulates ADSCs on skin flap survival

The specific functions of VEGFA regulating ADSCs on the perforator flap survival were also investigated. ADSCs were

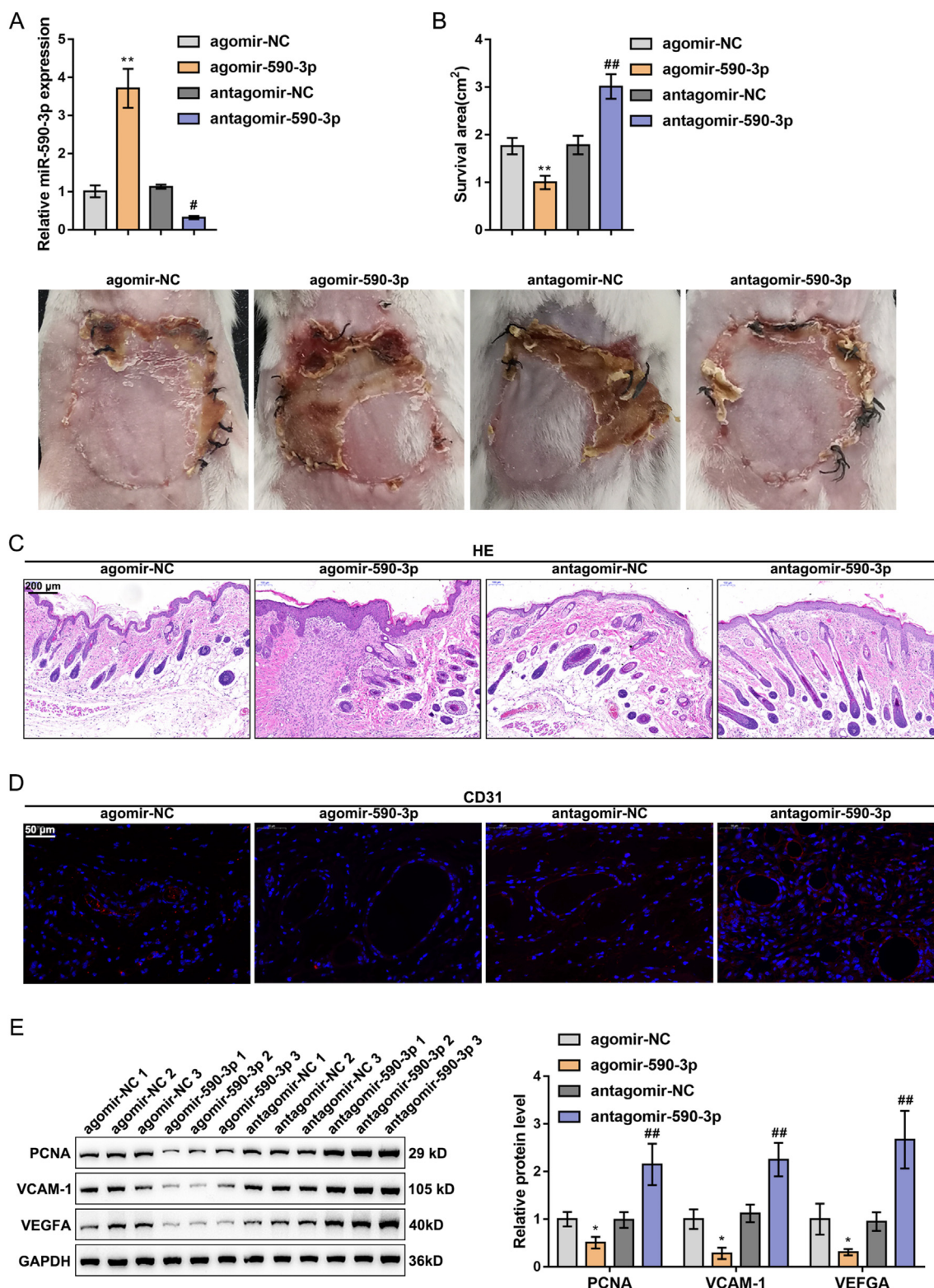


**Fig. 2.** The effect of miR-590-3p regulates ADSCs on skin flap survival (A) agomir-590-3p/antagomir-590-3p was transfected into ADSCs, with the transfection efficiency verified using PCR assay (B) The transfected ADSCs were injected into the skin flap mice subcutaneous tissue. Representative flap images on the 7th day after the operation and the survival area were analyzed (C) The assessment of skin tissue damage was applied by H&E staining (D) CD31 expression in skin tissue was detected by IF staining (E) PCNA, VCAM-1 and VEGFA levels were detected by Western blot. N = 5; \*P < 0.05, \*\*P < 0.01, compared with agomir-NC group; #P < 0.05, ##P < 0.01, compared with antagomir-NC group.

transfected with the interference vector of VEGFA or ADSCs plus VEGFA recombinant protein (rVEGFA) and subsequently injected into the skin flap mice. The knockdown of VEGFA significantly

inhibited, while rVEGFA notably promoted the survival of the perforator flap (Fig. 4A). H&E staining results showed that the skin tissues in the si-VEGFA group had sustained enlarged inflammation

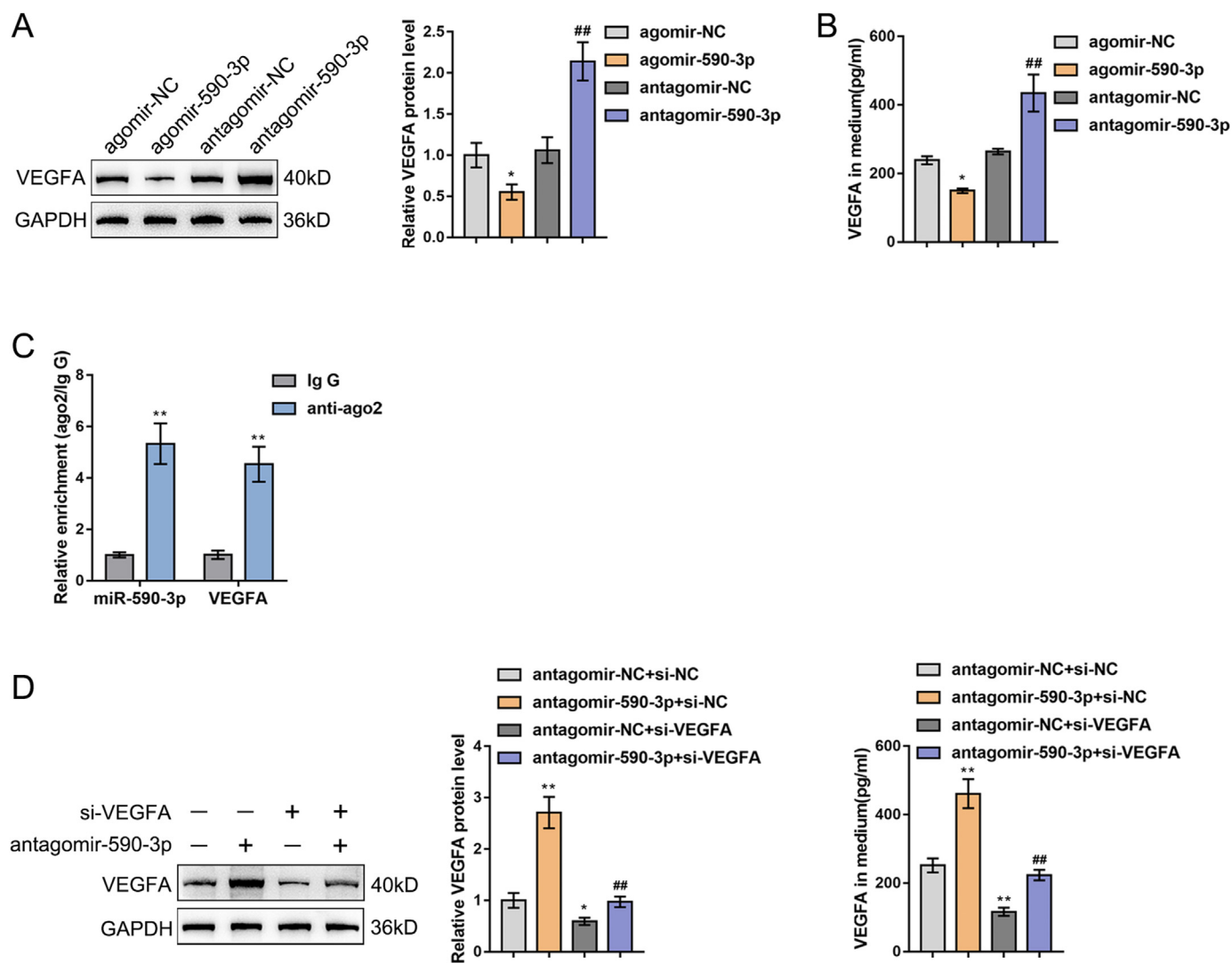


**Fig. 3. MiR-590-3p targeted VEGFA regulates its expression** (A–B) agomir-590-3p/antagomir-590-3p was transfected into ADSCs. VEGFA levels in cells were determined using Western blot (A). VEGFA levels in the culture medium were determined by ELISA assay (B). N = 3; \*P < 0.05, compared with agomir-NC group; ##P < 0.01, compared with antagomir-NC group (C) MiR-590-3p and VEGFA expressions were detected in ADSCs bound to the Ago2 antibody or IgG by RIP assay. N = 3; \*\*P < 0.01, compared with IgG group (D–E) agomir-590-3p and/or si-VEGFA were transfected into ADSCs and the VEGFA levels in cells and culture medium were examined using Western blot (left) and ELISA assay (right). N = 3; \*P < 0.05, \*\*P < 0.01, compared with antagomir-NC + si-NC group; ##P < 0.01 compared with antagomir-NC + si-VEGFA group.

areas, increased fragmentary epithelialization, and reduced hair follicles, while the exogenous VEGFA exerted opposite effects (Fig. 4B). IF staining displayed that VEGFA silencing observably inhibited, while rVEGFA protein promoted CD31 expression (Fig. 4C). The knockdown of VEGFA notably inhibited, while rVEGFA protein promoted PCNA and VCAM-1 protein levels (Fig. 4D).

#### 4. Discussion

Large skin flaps are usually required to ensure ample blood supply to repair large skin defects in plastic and reconstructive surgery [20]. Tissue expansion is a mature technique for producing well-vascularized cutaneous tissues [21]. Nevertheless, during the creation of larger flaps, most expanders experienced over-expansion, leading to thinner skin. Stem cell therapy was proven to be promising in improving skin flap viability [22].

ADSCs can be widely applied clinically due to their availability from liposuction aspirates and *in-vitro* culture. Moreover, they do not entail ethical problems of any sort as compared with other

stem cells [8]. ADSCs possess numerous advantages (abundant reserves, easy access, high proliferative capability, and low senescence, immunogenicity, and donor site incidence) over other source-derived stem cells (such as mesenchymal stem cells derived from bone marrow and endothelial progenitor cells) [23,24]. Specific functions of ADSCs in skin flaps have also been investigated [25]. Hasdemir et al. proposed that ADSCs enhance the survival of random pattern cutaneous flaps in skin having sustained radiation injuries [26]. Han et al. concluded that ADSCs increased skin flap survival under venous ischemia-reperfusion conditions. ADSCs' enhancement of skin flap survival was proven, which is consistent with a previous study [27]. Our data also revealed that ADSCs enhanced skin flap recovery, as well as elevated CD31-stained cell numbers and PCNA, VCAM-1, and VEGFA levels. ADSCs were conclusively shown to facilitate skin flap survival via promoting angiogenesis.

Numerous studies have stated that several miRNAs are involved in flap reconstruction. Anecdotal reports indicated that four miRNAs (miR-96, miR-193-3p, miR-210, and miR-21) exhibited

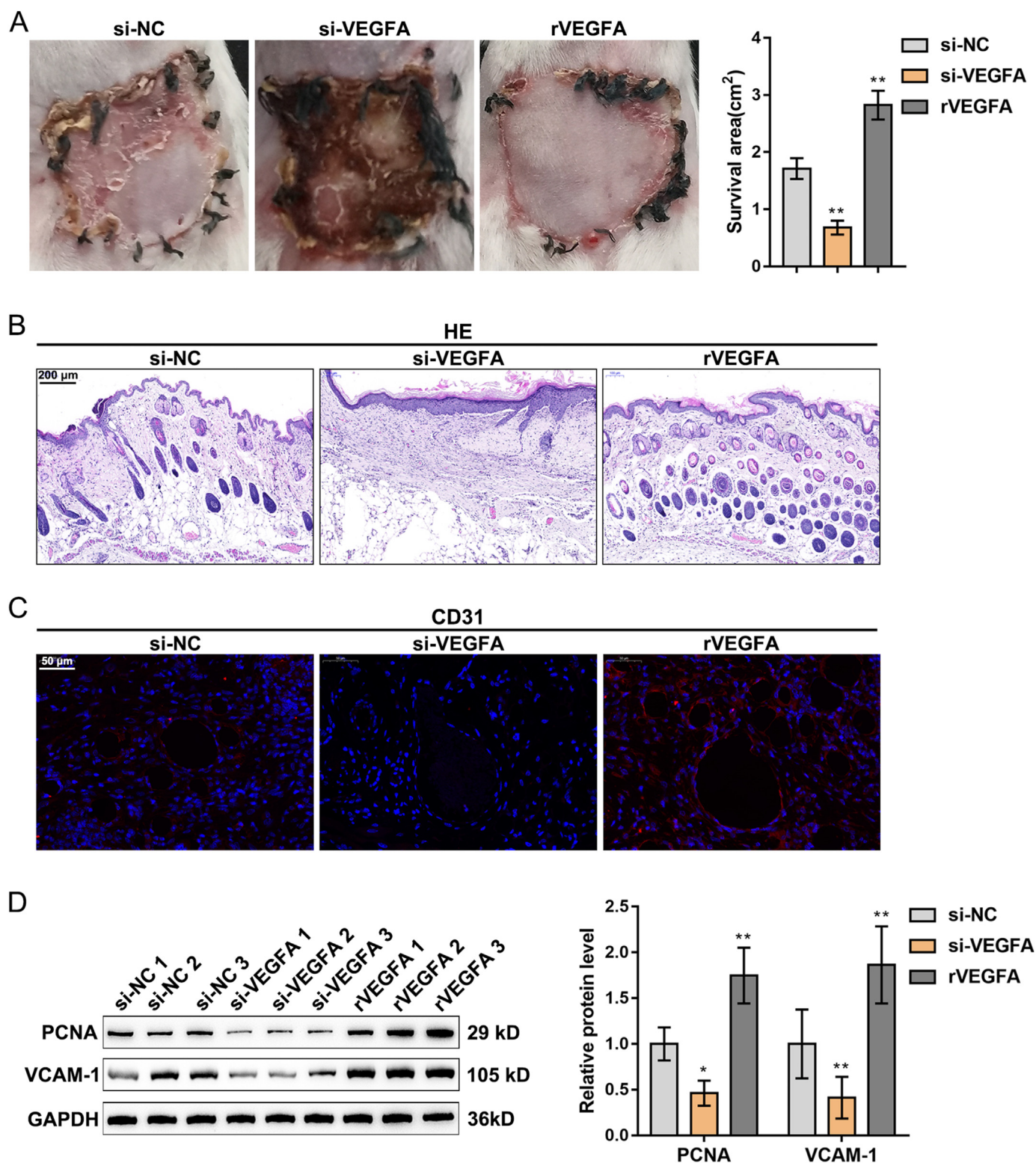


**Fig. 4.** The effect of VEGFA regulates ADSCs on skin flap survival. ADSCs were transfected with an interference vector of VEGFA (si-VEGFA) or mixed with 2 μg VEGFA recombinant protein (rVEGFA) and then injected into the skin flap mice (A) The representative images of flaps at post-operative day 7 were acquired and the survival area was analyzed (B) The assessment of skin tissue damage was applied by H&E staining (C) CD31 expression in skin tissue was detected by IF staining (D) PCNA and VCAM-1 levels in skin tissue were detected by Western blot. N = 5; \*P < 0.05, \*\*P < 0.01, compared with si-NC group.

upregulation in flap tissues after ischemia-reperfusion injury [28]. In a previous study, as analyzed by color laser Doppler imaging, miR-21-5p knockdown notably elevated rat skin flap angiogenesis and suppressed SMAD7 expression in ischemic skin tissues [29].

Specific functions of various miRNAs in ADSCs application have also been investigated. Zhang et al. suggested that miR-26a modulated ADSC adipogenic differentiation was induced by insulin through the regulation of the CDK5/FOXC2 pathway [30]. Li et al. concluded

that miR-5591-5p modulated ADSC impacts the repair of diabetic wounds by targeting the AGEs/AGER/JNK axis [31]. MiR-590-3p involved in this study has been verified to participate in the function exertion of ADSCs [18]. Nevertheless, little is known about miR-590-3p's biological functions in ADSCs in skin flap survival. This study demonstrated that miR-590-3p overexpression inhibited skin flap recovery by restricting the number of CD31 stained cells and PCNA, VCAM-1, and VEGFA levels.

The potential targeted gene was considered to further understand the underlying mechanism of miR-590-3p in ADSC application on the skin flap. As a transient entity, messenger RNA (mRNA) mediates genetic information translation from DNA-encoded genes to proteins in cells [32]. Vascular endothelial growth factor A (VEGFA) was the downstream targeted gene of miR-590-3p. VEGFA encodes a heparin-binding protein, which stimulates angiogenesis and vascular permeability [33]. In this study, exogenous VEGFA notably promoted the survival of perforator flap with ADSCs transplantation through the promotion of CD31, PCNA, and VCAM-1 expression. Similarly, previous studies also revealed VEGFA exerts crucial roles in skin flap. For example, Vourtsis et al. concluded that the administration of VEGFA improved the survival rate of the flap and thus contributed to the salvage of the greater peripheral segment of the flap [34]. Jafari et al. demonstrated that *in-vivo* electroporation-mediated gene transfer of VEGFA is a promising therapeutic approach to enhance the viability and vascularity of skin flap [35]. These outcomes demonstrate that VEGFA plays a protective role in the survival of skin flap.

## 5. Conclusion

The specific functions of ADSCs and miR-590-3p/VEGFA axis in skin flap survival were delineated. Our study assessed that ADSCs transplantation promotes skin flap survival by boosting angiogenesis. The miR-590-3p/VEGFA axis in ADSCs regulates angiogenesis and skin flap survival. These findings indicate that interfering with miR-590-3p expression in ADSCs may be considered a novel therapeutic strategy for the improvement of skin flap survival.

## Ethical statement

The animal studies were performed after receiving approval of the Institutional Animal Care and Use Committee (IACUC) in Central South University (IACUC approval No. 2021271).

## Declaration of competing interest

The authors declare that they have no competing interests.

## Acknowledgements

This study was supported by Hunan Provincial Science and Technology Innovation Plan Project-Provincial Key R&D Project (2018SK2086), Hunan Provincial Science and Technology Innovation Guidance Program Project (2020SK53417), Key Projects of Hunan Provincial Health Commission (20200048) and Natural Science Foundation of Hunan Province (2021JJ30034 and 2019JJ50847).

## Appendix A. Supplementary data

Supplementary data to this article can be found online at <https://doi.org/10.1016/j.reth.2022.07.010>.

## References

- [1] Chen L, Chen R, Guan Z, Lin P, Liang F, Han P, et al. Platysma skin flap: laryngeal repair material to produce phonatory flap vibrational wave. *Head Neck* 2020;42:2757–63.
- [2] Lucas JB. The physiology and biomechanics of skin flaps. *Facial Plast Surg Clin North Am* 2017;25:303–11.
- [3] Qiu D, Wang X, Wang X, Jiao Y, Li Y, Jiang D. Risk factors for necrosis of skin flap-like wounds after ED debridement and suture. *Am J Emerg Med* 2019;37:828–31.
- [4] Karimipour M, Hassanzadeh M, Zirak Javanmard M, Farjah G. Oral administration of alanyl-glutamine and glutamine improve random pattern dorsal skin flap survival in rats. *Iran J Basic Med Sci* 2018;21:842–7.
- [5] Li W, Enomoto M, Ukegawa M, Hirai T, Sotome S, Wakabayashi Y, et al. Subcutaneous injections of platelet-rich plasma into skin flaps modulate proangiogenic gene expression and improve survival rates. *Plast Reconstr Surg* 2012;129:858–66.
- [6] Ballestin A, Casado JG, Abellan E, Vela FJ, Alvarez V, Uson A, et al. Ischemia-reperfusion injury in a rat microvascular skin free flap model: a histological, genetic, and blood flow study. *PLoS One* 2018;13:e0209624.
- [7] Li Y, Jiang QL, Van der Merwe L, Lou DH, Lin C. Preclinical efficacy of stem cell therapy for skin flap: a systematic review and meta-analysis. *Stem Cell Res Ther* 2021;12:28.
- [8] Bacakova L, Zarubova J, Travnickova M, Musilkova J, Pajorova J, Slepicka P, et al. Stem cells: their source, potency and use in regenerative therapies with focus on adipose-derived stem cells - a review. *Biotechnol Adv* 2018;36:1111–26.
- [9] Sheykhkhan M, Wong JKL, Seifalian AM. Human adipose-derived stem cells with great therapeutic potential. *Curr Stem Cell Res Ther* 2019;14:532–48.
- [10] Klar AS, Zimoch J, Biedermann T. Skin tissue engineering: application of adipose-derived stem cells. *BioMed Res Int* 2017;2017:9747010.
- [11] Pu CM, Liu CW, Liang CJ, Yen YH, Chen SH, Jiang-Shieh YF, et al. Adipose-derived stem cells protect skin flaps against ischemia/reperfusion injury via IL-6 expression. *J Invest Dermatol* 2017;137:1353–62.
- [12] Reichenberger MA, Heimer S, Schaefer A, Lass U, Gebhard MM, Germann G, et al. Adipose derived stem cells protect skin flaps against ischemia-reperfusion injury. *Stem Cell Rev Rep* 2012;8:854–62.
- [13] Yu WY, Sun W, Yu DJ, Zhao TL, Wu LJ, Zhuang HR. Adipose-derived stem cells improve neovascularization in ischemic flaps in diabetic mellitus through HIF-1alpha/VEGF pathway. *Eur Rev Med Pharmacol Sci* 2018;22:10–6.
- [14] Pu CM, Chen YC, Chen YC, Lee TL, Peng YS, Chen SH, et al. Interleukin-6 from adipose-derived stem cells promotes tissue repair by the increase of cell proliferation and hair follicles in ischemia/reperfusion-treated skin flaps. *Mediat Inflamm* 2019;2019:2343867.
- [15] Lu TX, Rothenberg ME. MicroRNA. *J Allergy Clin Immunol* 2018;141:1202–7.
- [16] Shi R, Jin Y, Hu W, Lian W, Cao C, Han S, et al. Exosomes derived from mmu\_circ\_0000250-modified adipose-derived mesenchymal stem cells promote wound healing in diabetic mice by inducing miR-128-3p/SIRT1-mediated autophagy. *Am J Physiol Cell Physiol* 2020;318:C848–56.
- [17] Li X, Zhao Y, Li X, Wang Q, Ao Q, Wang X, et al. MicroRNA-150 modulates adipogenic differentiation of adipose-derived stem cells by targeting Notch3. *Stem Cell Int* 2019;2019:2743047.
- [18] Sun Y, Xiong X, Wang X. The miR-590-3p/VEGFA axis modulates secretion of VEGFA from adipose-derived stem cells, which acts as a paracrine regulator of human dermal microvascular endothelial cell angiogenesis. *Hum Cell* 2020;33:479–89.
- [19] Okşar HS, Coşkunfirat O, Ozgentaş H. Perforator-based flap in rats: a new experimental model. *Plast Reconstr Surg* 2001;108:125–31.
- [20] Hashimoto I, Abe Y, Ishida S, Kashiwagi K, Minoda K, Yamashita Y, et al. Development of skin flaps for reconstructive surgery: random pattern flap to perforator flap. *J Med Invest* 2016;63:159–62.
- [21] Marcus J, Horan DB, Robinson JK. Tissue expansion: past, present, and future. *J Am Acad Dermatol* 1990;23:813–25.
- [22] Ojeh N, Pastar I, Tomic-Canic M, Stojadinovic O. Stem cells in skin regeneration, wound healing, and their clinical applications. *Int J Mol Sci* 2015;16:25476–501.
- [23] Mazini L, Rochette L, Admou B, Amal S, Malka G. Hopes and limits of adipose-derived stem cells (ADSCs) and mesenchymal stem cells (MSCs) in wound healing. *Int J Mol Sci* 2020:21.
- [24] Ogawa R. Adipose-derived stem cells. *Curr Stem Cell Res Ther* 2010;5:94.
- [25] Foroglou P, Karathanasis V, Demiri E, Koliakos G, Papadakis M. Role of adipose-derived stromal cells in pedicle skin flap survival in experimental animal models. *World J Stem Cell* 2016;8:101–5.
- [26] Hasdemir M, Agir H, Eren GG, Aksu MG, Alagoz MS, Duruksu G, et al. Adipose-derived stem cells improve survival of random pattern cutaneous flaps in radiation damaged skin. *J Craniofac Surg* 2015;26:1450–5.
- [27] Han HH, Lim YM, Park SW, Lee SJ, Rhie JW, Lee JH. Improved skin flap survival in venous ischemia-reperfusion injury with the use of adipose-derived stem cells. *Microsurgery* 2015;35:645–52.



- [28] Chang KP, Lai CS. Micro-RNA profiling as biomarkers in flap ischemia-reperfusion injury. *Microsurgery* 2012;32:642–8.
- [29] Chang CH, Yen MC, Liao SH, Hsu YL, Lai CS, Kuo YR, et al. Dual role of MiR-21-mediated signaling in HUVECs and rat surgical flap under normoxia and hypoxia condition. *Int J Mol Sci* 2017;18.
- [30] Zhang XX, Wang YM, Su YD, Zuo F, Wu B, Nian X. Correction to: MiR-26a regulated adipogenic differentiation of ADSCs induced by insulin through CDK5/FOXO2 pathway. *Mol Cell Biochem* 2021;476:3217.
- [31] Li Q, Xia S, Yin Y, Guo Y, Chen F, Jin P. miR-5591-5p regulates the effect of ADSCs in repairing diabetic wound via targeting AGEs/AGER/JNK signaling axis. *Cell Death Dis* 2018;9:566.
- [32] Zhao BS, Roundtree IA, He C. Post-transcriptional gene regulation by mRNA modifications. *Nat Rev Mol Cell Biol* 2017;18:31–42.
- [33] Karaman S, Leppanen VM, Alitalo K. Vascular endothelial growth factor signaling in development and disease. *Development* 2018:145.
- [34] Vourtsis SA, Spyriounis PK, Agrogiannis GD, Ionac M, Papalois AE. VEGF application on rat skin flap survival. *J Invest Surg* 2012;25:14–9.
- [35] Seyed Jafari SM, Blank F, Ramser HE, Woessner AE, Shafiqhi M, Geiser T, et al. Efficacy of combined in-vivo electroporation-mediated gene transfer of VEGF, HGF, and IL-10 on skin flap survival, monitored by label-free optical imaging: a feasibility study. *Front Surg* 2021;8: 639661.